

Active Disturbance Rejection and PID Control of a One-stage Refrigeration Cycle

J.J. Carreño-Zagarra* R. Villamizar* J.C. Moreno**
J.L. Guzmán**

* *Universidad Industrial de Santander, Bucaramanga, Colombia, 680002 (e-mail: jose.carreno@correo.uis.edu.co, rovillam@uis.edu.co).*

** *Universidad de Almería, CIESOL, ceiA3, Almería, Spain, 04120 (e-mail: jcmoreno@ual.es, joguzman@ual.es)*

Abstract: This document addresses the problem of controlling a one-stage refrigeration cycle by using the opening of the expansion valve and the compressor speed as control variables, while the outlet temperature of evaporator secondary flux and the superheating degree of refrigerant at evaporator outlet are the controlled variables. An uncertain matrix function is obtained in order to represent the full operating range of the nonlinear system. Thus, the control decentralized approach control consists of designing Generalized- Proportional-Integral (GPI) observers for the internal loops of each controlled variable while PID controllers are tuned based on the Quantitative Feedback Theory for the respective external loops. Simulations results show that the robust controllers reacts quickly reference settings, despite the non-measurement of the disturbance variables and the dynamic coupling of the multi-variable system, compared to decentralised single PIDs proposed with the benchmark.

Keywords: Refrigeration system, Vapour compression cycle, Active disturbance rejection, Quantitative feedback theory, Decoupling control, Robust control.

1. INTRODUCTION

Most of domestic or industrial air conditioning and refrigeration systems use steam compression cycles, which demand a high energy consumption and their economic and environmental impact is well characterized (Bejarano et al., 2015). Thus, by improving the efficiency of these systems a potential economic and environmental impact will be achieved. This implies not only refining designs of individual components, but also increasing the overall efficiency of the system by means of advanced control strategies (Rasmussen, 2005).

Refrigeration by steam compression is one of the most used technologies worldwide for generating cold, more in industrial than domestic refrigeration (Rasmussen, 2005). The power demand range varies from 1 kW to 1 MW which implies a high energy consumption and consequently a strong impact on economic and environmental balances. For example, supermarkets -which are high energy consumers- consume between 2 and 3 MW per year and around 50% of this energy is consumed in the cooling processes. In addition, approximately 30% of total energy all over the world is consumed for ventilating, heating and air conditioning (HVAC systems), as well as refrigerators and water heaters (Jahangeer et al., 2011). Specifically, some studies remark that air conditioners and refrigerators involve 28% of home

energy consumption in USA (Bejarano et al., 2017). Thus, by improving the energy efficiency in the refrigeration cycle can potentially lead to a significant reduction in energy consumption.

On the other hand, steam compression refrigeration systems are highly non-linear multivariable systems, with cross-coupling variables, thus their dynamic modelling is not trivial. Due to the advance of the electronics industry, variable speed compressors and electronic expansion valves have progressively replaced older single speed compressors and thermostatic expansion valves, respectively. This has allowed designing smarter control strategies, for not only saving energy but also for mitigating fluctuations in the controlled variables and therefore obtaining a more accurate control and a better system performance.

Some of the most used linear control techniques for this kind of problems are model predictive control, decoupling multivariate control, LQG control, robust control H_∞ and PID control. The main advantage of using PID controllers is their easy tuning and implementation, while the main advantage of most advanced controllers is their dynamic performance. However, the interactions or cross-coupling among various input and outputs, the external disturbance and the parametric uncertainty of these systems makes it difficult to tune PID controllers.

Active Disturbance Rejection Control (ADRC) is a mature technique for controlling both linear and non-linear uncertain systems (Sira-Ramírez et al., 2011), that accounts external disturbances and the dynamic cross-coupling problem. Its main goal is to estimate the unknown system

* This work has been partially funded by Departamento Administrativo de Ciencia, Tecnología e Innovación (Colombia) and by the following projects: DPI2014-55932-C2-1-R, DPI2014-56364-C2-1-R and DPI2017-84259-C2-1-R (financed by the Spanish Ministry of Economy, Industry and Competitiveness and EU-ERDF funds).

dynamics in order to control and suppress its effect by complementing the control law with a cancellation effort. Such estimations can be carried out by linear observers called: Generalized Integral Proportional (GPI) observers. This control law can be naturally applied to differentially flat nonlinear systems, which are a prominent and frequent class of non-linear systems (Fliess et al., 1995).

In this paper the stated robust control problem is solved for a one-stage refrigeration cycle using the active disturbance rejection approach through the design of GPI observers in the internal control loops and PID controllers in the external loops by means of QFT methodology (Horowitz, 1982). Firstly, section 2 presents the identification of multivariable linear models at different operating points by means of step response, in order to describe the fundamental full dynamic behaviour of the system. Section 3 describes the design of GPI observers and robust PID controllers that meet stability, sensitivity and reference tracking specifications at all frequencies of interest for the uncertain model. Section 4 shows the validation results and its respective analysis. Finally, section 5 presents the main conclusions.

2. PROCESS MODEL

According to Fig. 1, a refrigeration cycle consists of: i) variable-speed compressor, ii) electronic expansion valve, iii) evaporator and iv) condenser, where the objective of each cycle is to remove heat from the secondary flux at the evaporator and reject heat at the condenser by transferring it to the secondary flux. The inverse Rankine cycle is applied, where the refrigerant enters the evaporator at a low temperature and pressure and it evaporates while removing heat from the evaporator secondary flux. Then, the compressor increases the refrigerant pressure and temperature, and it enters to the condenser, where first its temperature decreases, secondly condenses and finally becomes subcooled liquid while transferring heat to the condenser secondary flux. The expansion valve closes the cycle by upholding the pressure difference between the condenser and the evaporator.

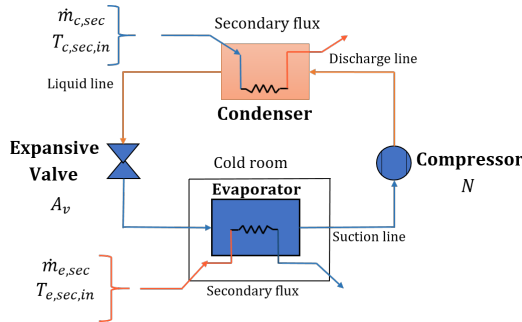


Fig. 1. Vapour compression system

A large variety of refrigeration cycle system models can be found: from very complex ones to simple models. These last oriented to multivariable control strategies. The dynamical model used in this work is inspired in (Li and Alleyne, 2010). The heat exchangers are modelled using the switched moving boundary method (Rasmussen, 2005), where the heat exchanging zone is split into variable-length

subzones of superheated, two-phase or/and subcooled refrigerant. According to the number and type of existing subzones, up to five model representations or modes for the condenser and two modes for the evaporator are defined.

For every mode, the state vectors \mathbf{x}_c and \mathbf{x}_e in (1) gather the most relevant information at each instant of condenser and evaporator, respectively.

$$\begin{aligned}\mathbf{x}_c &= [h_{c,sh} \ P_c \ h_{c,sc} \ \zeta_{c,sh} \ \zeta_{c,tp} \ \gamma_c]^T \\ \mathbf{x}_e &= [\zeta_{e,tp} \ P_e \ h_{e,sh} \ \gamma_e]^T \\ \mathbf{x}_{cycle} &= [\mathbf{x}_c \ \mathbf{x}_e]^T\end{aligned}\quad (1)$$

The state vectors \mathbf{x}_e and \mathbf{x}_c contain heterogeneous variables such as the evaporation and condensation pressures, P_e and P_c , specific enthalpies describing the single-phase zones such as $h_{c,sh}$, $h_{c,sc}$ and $h_{e,sh}$, the zone lengths $\zeta_{c,sh}$, $\zeta_{c,tp}$ and $\zeta_{e,tp}$, and the mean void fractions at both heat exchangers γ_c and γ_e (Bejarano et al., 2017).

The uniform state vectors enable the different heat exchanger modes to retain a constant dynamical system structure formulated in the nonlinear descriptor form shown in (2) (Alfaya et al., 2015):

$$\begin{aligned}\mathbf{Z}_c(\mathbf{x}_c, \mathbf{u}_c) \dot{\mathbf{x}}_c &= \mathbf{f}_c(\mathbf{x}_c, \mathbf{u}_c) \\ \mathbf{Z}_e(\mathbf{x}_e, \mathbf{u}_e) \dot{\mathbf{x}}_e &= \mathbf{f}_e(\mathbf{x}_e, \mathbf{u}_e)\end{aligned}\quad (2)$$

Each mode in both heat exchangers has its own coefficient matrix $\mathbf{Z}(\mathbf{x}, \mathbf{u})$, forcing function $\mathbf{f}(\mathbf{x}, \mathbf{u})$ for storing thermodynamic variables, and mass and energy balance terms (Alfaya et al., 2015). The choice of model outputs will depend on the interfaces with other system components models:

$$\begin{aligned}\mathbf{u}_c &= [\dot{m}_{c,sec} \ T_{c,sec,in} \ \dot{m}_{c,in} \ \dot{m}_{c,out} \ h_{c,in}]^T \\ \mathbf{u}_e &= [\dot{m}_{e,sec} \ T_{e,sec,in} \ \dot{m}_{e,in} \ \dot{m}_{e,out} \ h_{e,in}]^T\end{aligned}\quad (3)$$

where \dot{m} is the mass flow and T is the temperature. The subscripts are defined as: c : condenser, e : evaporator, sec : secondary flux, in : inlet and out : outlet.

In this work neither the mass flow $\dot{m}_{e,sec}$ nor the inlet temperature $T_{e,sec,in}$ are intended to be controlled. Therefore, the cooling demand can be expressed as a reference on the outlet temperature of the evaporator secondary flux $T_{e,sec,out}$, where the mass flow and inlet temperature act as measurable disturbances. Regarding the condenser, the inlet temperature $T_{e,sec,in}$ and mass flow $\dot{m}_{c,sec}$ of the secondary flux are also considered as disturbances. The manipulated variables are the compressor speed N and the expansion valve opening A_v .

2.1 Uncertain linear model

In order to describe the fundamental dynamic behaviour of the refrigerator system and to design the robust controller, linear models were identified at different operating points by means of a step response. Each model is expressed in the continuous transfer matrix form:

$$\begin{bmatrix} \Delta T_{e,sec,out}(s) \\ \Delta T_{SH}(s) \end{bmatrix} = G(s) \begin{bmatrix} \Delta A_v(s) \\ \Delta N(s) \end{bmatrix}\quad (4)$$

where,

$$G(s) = \begin{bmatrix} G_{11}(s) & G_{12}(s) \\ G_{21}(s) & G_{22}(s) \end{bmatrix} \quad (5)$$

and

$$G_{ij} = \frac{k_{ij} (T_{z_{ij}} s + 1)}{(\tau_{p_{ij}} s + 1) (T_{f_{ij}} s + 1)}; \quad i, j = 1, 2. \quad (6)$$

The fixed parameters of the obtained model are the following:

$$\begin{aligned} \tau_{p_{11}} &= 26.133, \tau_{p_{12}} = 30.494, \tau_{p_{21}} = 27.5, \tau_{p_{22}} = 39.927, \\ T_{z_{11}} &= 42.6, T_{z_{12}} = 9.1954, T_{z_{21}} = 38.6, T_{z_{22}} = 52.675. \end{aligned}$$

And the uncertain parameters of the dynamic model are the following:

$$\begin{aligned} k_{11} &= [-0.02532, -0.015204], k_{12} = [-1.96, -1.49] 10^{-3} \\ k_{21} &= [-0.407, -0.229], k_{22} = [0.137, 0.172] \\ T_{f_{11}} &= [0.1, 0.27], T_{f_{12}} = [0.25, 0.57], \\ T_{f_{21}} &= [0.0146, 0.247], T_{f_{22}} = [5.76, 7.68] 10^{-2}. \end{aligned}$$

The so-called fixed parameters were kept constant at the different points of operation of the identification process while the so-called uncertain parameters changed in value in each test. Table 1 includes the accepted range of the input variables, used in the identification of the uncertain parameters model.

Table 1. Input variable ranges

Variable	Range	Units
A_v	[10, 100]	%
N	[30, 50]	Hz
$T_{c,sec,in}$	[27, 33]	$^{\circ}C$
$T_{e,sec,in}$	[-22, -18]	$^{\circ}C$
T_{surr}	[20, 30]	$^{\circ}C$
$\dot{m}_{c,sec}$	[125, 175]	gs^{-1}
$\dot{m}_{e,sec}$	[0.0075, 0.055]	gs^{-1}
$P_{c,sec,in}$	-	bar
$P_{e,sec,in}$	-	bar

3. CONTROLLERS DESIGN

This section presents the design of both the disturbance observer based on differential flatness and the robust PID controller within a two-degrees-of-freedom control scheme.

3.1 Active Disturbance Rejection

Consider a single-input single-output linear system, depicted by the following frequency domain form:

$$y(s) = P_r(s) [u(s) + d(s)] \quad (7)$$

where $u(s)$ is the control input, $y(s)$ the controlled output, $d(s)$ the external disturbance, and $P_r(s)$ the real plant.

Fig. 2 presents the blocks diagram for the disturbance observer, in the frequency domain, for system described by (7), where $Q(s)$ is the disturbance filter.

The transfer function of the equivalent plant with input $u(t)$ and output $y(t)$:

$$P_{eq}(s) = \frac{P_r(s)}{1 - Q(s) + D_{\hat{d}y}(s)P_r(s)} \quad (8)$$

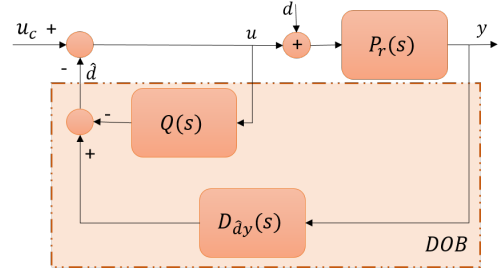


Fig. 2. Blocks diagram of disturbance observer

In order to achieve that $P_{eq}(s) \approx P_r(s)$ it must be guaranteed that:

$$D_{\hat{d}y}(s) = Q(s)P_n^{-1}(s) \quad (9)$$

Where, $P_n(s)$ is the nominal plant.

In this way, the transfer function is described as follows:

$$P_{eq}(s) = \frac{P_r(s)}{1 - Q(s) \left(1 - \frac{P_r(s)}{P_n(s)}\right)} \quad (10)$$

Lets consider the estimated disturbance signal, in order to show how the observer estimates the disturbances (external and internal):

$$\hat{d}(s) = D_{\hat{d}y}(s)y(s) - Q(s)u(s) \quad (11)$$

By substituting (7) and (9) in (11), it is obtained that:

$$\hat{d}(s) = d(s)Q P_r P_n^{-1} - Q [(1 - P_r P_n^{-1}) u(s)] \quad (12)$$

When $\lim_{s \rightarrow 0} Q(s) [(1 - P_r P_n^{-1}) u(s)] \approx 0$, the disturbance estimation error can be approximated as:

$$e_d(s) = \hat{d}(s) - d(s) \approx d(s)(Q(s) - 1) \quad (13)$$

The disturbance estimation error $e_d(s)$ will trend to zero as time goes to infinity, if the filter $Q(s)$ is selected as a low-pass form: that is, $\lim_{s \rightarrow 0} Q(s) = 1$.

3.2 GPI Observer Design

Consider the n-dimensional, smooth dynamic system:

$$y^{(n)} = K(t, y)u + \psi(t) \quad (14)$$

where $K(t, y)$ is known, evenly bounded and far from zero, and the function $\psi(t)$ can be unknown and is uniformly absolutely bounded as well as all and each of its temporal derivatives to a finite order m . Lets consider the following observer of grade $n + m$:

$$\begin{aligned} \dot{y}_0 &= y_1 + \lambda_{m+n-1}(y - y_0) \\ \dot{y}_j &= y_{j+1} + \lambda_{m+n-j-1}(y - y_0), \\ & \quad j = 1, \dots, n - 2 \\ \dot{y}_{n-1} &= K_n u + z_1 + \lambda_m(y - y_0) \\ \dot{z}_l &= z_{l+1} + \lambda_{m-l}(y - y_0), \quad l = 1, 2, \dots, m - 1 \\ \dot{z}_m &= \lambda_0(y - y_0) \end{aligned} \quad (15)$$

$$Q(s) = \frac{\lambda_{m-1}s^{m-1} + \lambda_{m-2}s^{m-2} + \dots + \lambda_0}{s^{n+m} + \lambda_{n+m-1}s^{n+m-1} + \dots + \lambda_0} \quad (16)$$

This observer is commonly called as Generalized Proportional Integral (GPI) and the disturbance estimation error

can be reduced as small as desired if the observer gain parameters $\{\lambda_0, \dots, \lambda_{m+n-1}\}$ are appropriately selected. The coefficients λ_j are selected such that the following polynomial in the complex variable s , is Hurwitz:

$$p_{obs}(s) = s^{m+n} + \lambda_{m+n-1}s^{m+n-1} + \dots + \lambda_0 = 0 \quad (17)$$

By using the methodology proposed by (Keel et al., 2008), in order to mitigate typical peaking effects in high gain observers, the coefficient λ_0 can be chosen as:

$$\lambda_0 = \frac{T\alpha_0}{\lambda_{n+m}} \quad (18)$$

where α_0 is an arbitrary and strictly positive constant and the term $T > 0$ is known as the desired settling time or generalized time constant. The parameters $\lambda_0, \lambda_1 \dots \lambda_{n+m}$ are determined by:

$$\lambda_i = \frac{T^i \alpha_0}{\alpha_{i-1} \alpha_{i-2}^2 \alpha_{i-3}^3 \dots \alpha_1^{i-1} \lambda_{n+m}}, i = 1, \dots, n+m-1 \quad (19)$$

$$\lambda_{n+m} = \frac{T^{n+m} \alpha_0}{\alpha_{n+m-1} \alpha_{n+m-2}^2 \alpha_{n+m-3}^3 \dots \alpha_1^{n+m-1}} \quad (20)$$

From the above expressions, α_1 is the desired damping factor of the observer and it must be an adjustable constant parameter greater than 2. (Keel et al., 2008) proposes to calculate the remaining α_k coefficients by:

$$\alpha_k = \alpha_1 \frac{\sin\left(\frac{k\pi}{n+m}\right) + \sin\left(\frac{\pi}{n+m}\right)}{2 \sin\left(\frac{k\pi}{n+m}\right)}, k = 2, \dots, n+m-1 \quad (21)$$

3.3 QFT controller design

The quantitative feedback theory (QFT) is a robust control strategy that proposes explicitly the use of feedback to reduce the effects of plant uncertainty and satisfy desired performance control specifications using a 2DOF control scheme (Horowitz, 1982). This method searches quantitatively for a controller that satisfies all the required performance specifications for every plant within the uncertain parameters set.

The specifications set is given by:

Stability specification:

$$\left| \frac{y(j\omega)}{F(j\omega)r(j\omega)} \right| = \left| \frac{K(j\omega)P(j\omega)}{1 + K(j\omega)P(j\omega)H(j\omega)} \right| \leq \delta_U(\omega) \quad (22)$$

Where $K(j\omega)$ is the controller, $P(j\omega)$ is the plant and $H(j\omega)$ is the transfer function of the sensor.

The stability specification has to be achieved at every frequency of interest, where this inequality imposes a maximum over-impulse in closed-loop system response. It also guarantees minimum phase and gain margins, which reflects the degree of stability of the control system.

Disturbance rejection at plant output:

$$\left| \frac{y(j\omega)}{d_o(j\omega)} \right| = \left| \frac{1}{1 + K(j\omega)P(j\omega)H(j\omega)} \right| \leq \delta_s(j\omega) \quad (23)$$

Unlike the stability, the sensitivity specification $\delta_s(\omega)$ is usually defined only for some low to middle frequencies. In this way, the high frequency activity of the actuators is reduced and possible mechanical fatigue problems are avoided. A practical selection of $\delta_s(\omega)$ is shown in (24). The

specification has also a slope of $-20dB/dec$ that reaches the $-3dB$ level at the frequency $\omega = a_d$, and has a 0 value for high frequency (Garcia-Sanz, 2017).

$$\delta_s(s) = \frac{s}{s + a_d} \quad (24)$$

Reference tracking specification:

$$T_L(j\omega) \leq \left| \frac{y(j\omega)}{r(j\omega)} \right| = \left| \frac{F(j\omega)K(j\omega)P(j\omega)}{1 + K(j\omega)P(j\omega)} \right| \leq T_U(j\omega) \quad (25)$$

In order to reduce the high frequency activity of the actuators and avoid possible mechanical fatigue problems, the reference tracking specifications are generally defined only for some low to mid frequencies. A practical choice is given by the following expressions (Garcia-Sanz, 2017):

$$T_U(s) = \frac{\omega_n^2/a(s+a)}{s^2 + 2\zeta\omega_n s + \omega_n^2} \quad (26)$$

$$T_L(s) = \frac{1}{(\tau_1 s + 1)(\tau_2 s + 1)(\tau_3 s + 1)} \quad (27)$$

4. RESULTS

For the design and validation of the controller, an operation point is selected within the uncertainty of the plant model. Let $P_r(s, \theta)$ be the transfer function of the plant with uncertainty θ , the nominal plant is given by:

$$P_n(s) = P_r(s, \theta_n) \quad (28)$$

where θ_n is the parameters vector of the operation point, which was selected as:

$$\theta_n = \frac{\theta_{max} + \theta_{min}}{2} \quad (29)$$

where θ_{min} and θ_{max} are the lower and the upper parameters vector, respectively, of the uncertainty set.

In order to analyse the interaction of the inputs and outputs of the system, the Bristol relative gain matrix is used, which is defined by:

$$R = P_n(0) * P_n^{-T}(0) \quad (30)$$

In the case of the selected nominal plant, the obtained result is:

$$R = \begin{bmatrix} 0.85 & 0.15 \\ 0.15 & 0.85 \end{bmatrix} \quad (31)$$

This indicates that the pairs input-output $u_1 - y_1$ and $u_2 - y_2$ should be taken to perform the design of two single-input & single-output (SISO) controllers.

4.1 Selection of observer, filter and controller parameters

The observer gain parameters of both SISO systems were established as: $T = 6$, $\alpha_0 = 4$, $\alpha_1 = 4$ and $m = 3$ in (18)-(21).

Table 2 shows the stability, sensitivity and reference tracking specifications given by (22), (24), (26) and (27) for the equivalent plants $P(s)$ of $G_{11}(s)$ and $G_{22}(s)$. By using loop shaping on the Nichols chart with bounds computed from the template of the equivalent plant, the 2DOF controller is obtained as follows:

$$K(s) = K_p + \frac{K_i}{s} + \frac{K_d s}{(s/\beta + 1)} \quad (32)$$

$$F(s) = \frac{1}{\lambda s + 1} \quad (33)$$

Table 3 shows the controller and filter parameters for each SISO system.

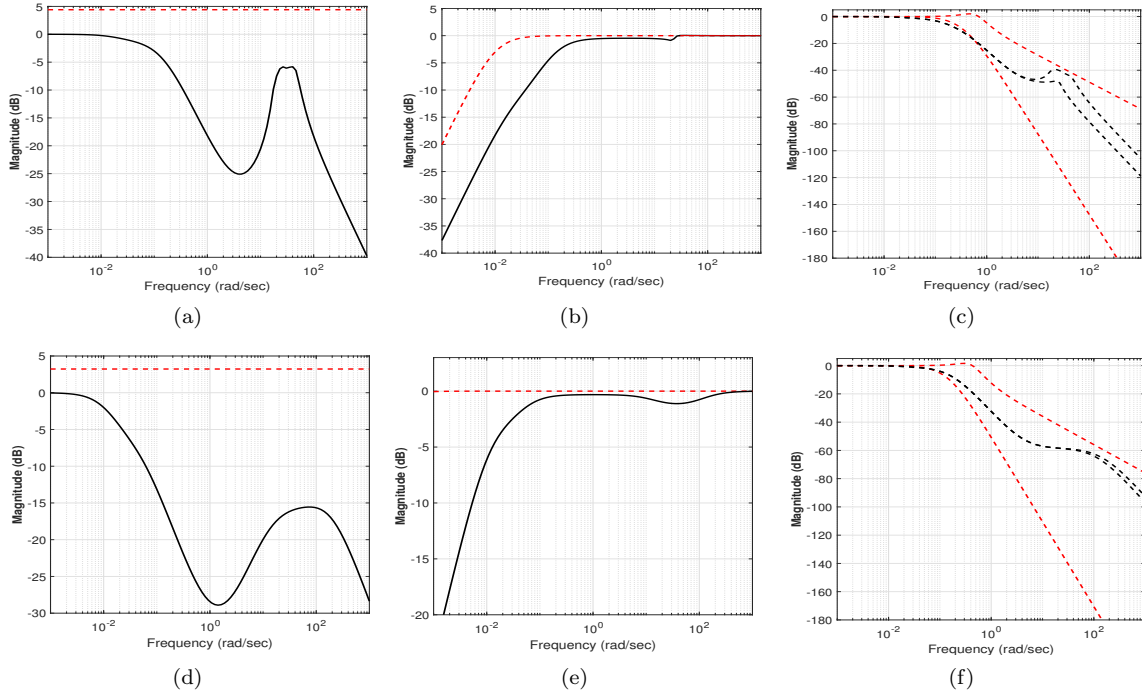


Fig. 3. Analysis of performance specifications. Stability: (a) $G_{11}(s)$, (d) $G_{22}(s)$; Disturbance rejection: (b) $G_{11}(s)$, (e) $G_{22}(s)$; Reference tracking: (c) $G_{11}(s)$, (f) $G_{22}(s)$. Specification (dashed line) and worst case within the uncertain plants at each frequency (solid line).

Table 2. Performance specifications

Parameter	For $G_{11}(s)$	For $G_{22}(s)$
δ_U	1.66	1.45
a_d	0.01	0.0001
ω_n	0.6	0.2
ζ	0.5	0.5
a	1	1
τ_1	2	6
τ_2	3	7
τ_3	4	8

Table 3. Parameters of filters and controller

Parameter	For $G_{11}(s)$	For $G_{22}(s)$
K_p	-2.2	1.44
K_i	-5	1
K_d	-0.228	0.41
β	100	16
λ	2	5

4.2 Validation Results and Analysis

Fig. 3 shows the stability, sensibility and tracking reference analysis in the frequency domain, where the dashed line is the specification in the frequency domain and the solid line in each plot represents the worst case. Fig. 3(a) presents the analysis of the closed-loop stability specification, defined in (22), for $G_{11}(s)$ and Fig. 3(d) for $G_{22}(s)$. The control system meets the stability specification since the solid line is below the dashed line δ_U in all the analysed cases.

Fig. 3(b) shows the frequency-domain analysis of the sensitivity specification for $G_{11}(s)$ and Fig. 3(e) for $G_{22}(s)$. The control system meets the sensitivity specification in all the studied cases, since the solid line is below the dashed line δ_s . Fig. 3(c) and Fig. 3(f) present the limits $T_L(j\omega)$ and $T_U(j\omega)$ in (25) in order to analyse the reference

tracking specification in the time-domain. It is observed that the control system meets the specification (is between the upper and lower limits) in all the studied cases.

On other hand, Fig. 4 shows the reference tracking of the controlled variables T_{SH} and $T_{sec, evap, out}$ within the considered range. Fig. 4(a) plots the manipulated variables, corresponding to A_v and N . It can be seen in Figure 4(b) that the PID controller with disturbance observer reacts quickly to the reference changes, despite the non-measurement of the perturbation variables and the existing dynamic coupling of the multivariable system.

In order to carry out a quantitative comparison between the two controllers, the average of eight performance indices is evaluated. The first two indices are the Ratios of Integrated Absolute Error (RIAE), taking into account that both the outlet temperature of evaporator secondary flux $T_{sec, evap, out}$ and the degree of superheating (T_{SH}) should follow their respective references. The third is the Ratio of Integrated Time multiplied Absolute Error (RITAE) for the first controlled variable $T_{sec, evap, out}$, taking into account that the standard simulation only includes one sudden change in its reference. The fourth, fifth, and sixth indices are the Ratios of Integrated Time multiplied Absolute Error (RITAE) for the second controlled variable (T_{SH}), taking into account that the standard simulation includes three sudden changes in its reference. The seventh and eighth indices are the Ratios of Integrated Absolute Variation of Control signal (RIAVU) for the two manipulated variables, the valve opening A_v and the compressor speed N . The combined index is obtained as the average value of the eight individual indices. Therefore, the combined performance index is described by:

$$J(C_1, C_2) = \frac{1}{8} \sum_{i=1}^8 R_i(C_1, C_2) \quad (34)$$

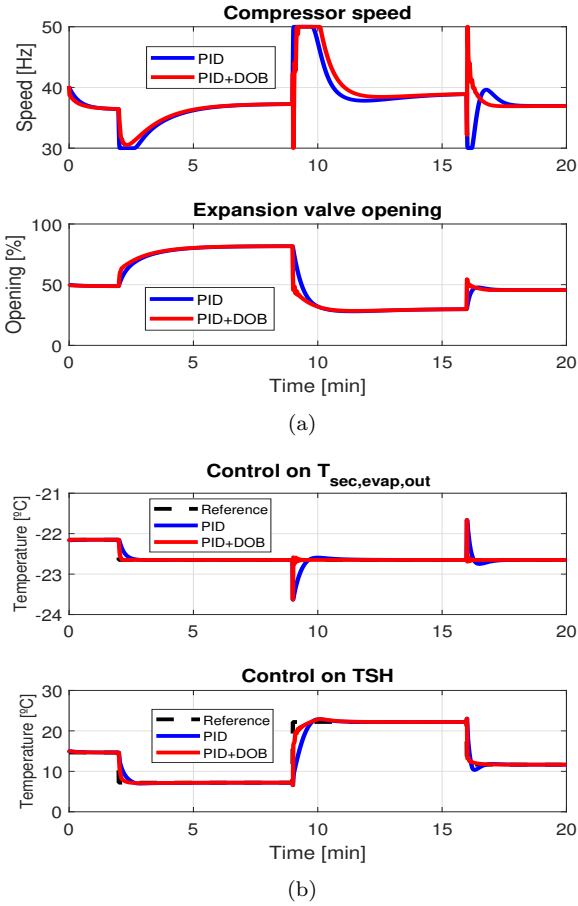


Fig. 4. Comparison of the decentralized PID controller with the ADCR-PID controller: (a) Input variables; (b) Output variables.

where each R_i (C_1, C_2) is the ratio between the i -th performance index of C_2 (PID controller with observer) and the i -th performance index C_1 (PID controller without observer). These indices are presented in the following expressions:

$$\begin{aligned}
 IAE_i &= \int_0^{time} |e_i(t)| dt \\
 ITAE_i &= \int_{t_c}^{t_c+t_s} (t - t_c) |e_i(t)| dt \\
 IAVU_i &= \int_0^{time} \left| \frac{du_i(t)}{dt} \right| dt
 \end{aligned} \quad (35)$$

Since the index $J(C_1, C_2)$ in (34) is equal to 0.4, the PID controller with GPI observer has a better performance than the reference controller.

5. CONCLUSIONS

In this paper the problem of robust control of a one-stage refrigeration cycle is solved by using GPI observers designed and robust PID controllers designed by means of QFT methodology. The efficiency of the observer is

due to the fact that the unknown parameters and external perturbations of the flat input-output dynamics are considered as an added additive perturbation, which is a function of time with the assumption of being absolutely uniformly bounded. This non-linear perturbation, as well as the phase variables associated with the flat output, are sufficiently accurately estimated in line by means of linear high-gain Luenberger observers, called GPI observers.

The proposed method is easy to implement, making it an appealing solution for refrigeration systems. Reference tracking analysis and a combined performance index shown that the robust controller reacts quickly to the reference changes, despite the non-measurement of the disturbance variables and the dynamic coupling of the multi-variable system, compared to decentralised PIDs proposed with the benchmark. In addition, stability and sensitivity specifications are reached throughout the range of uncertainty of the identified model.

REFERENCES

- Alfaya, J.A., Bejarano, G., Ortega, M.G., and Rubio, F.R. (2015). Controllability analysis and robust control of a one-stage refrigeration system. *European Journal of Control*, 26, 53–62.
- Bejarano, G., Alfaya, J.A., Ortega, M.G., and Rubio, F.R. (2015). Design, automation and control of a two-stage, two-load-demand experimental refrigeration plant. In *Control and Automation (MED), 2015 23th Mediterranean Conference on*, 537–544. IEEE.
- Bejarano, G., Alfaya, J.A., Ortega, M.G., and Vargas, M. (2017). On the difficulty of globally optimally controlling refrigeration systems. *Applied Thermal Engineering*, 111, 1143–1157.
- Fliess, M., Lévine, J., Martin, P., and Rouchon, P. (1995). Flatness and defect of non-linear systems: introductory theory and examples. *International journal of control*, 61(6), 1327–1361.
- Garcia-Sanz, M. (2017). *Robust control engineering: practical QFT solutions*. CRC Press.
- Horowitz, I. (1982). Quantitative feedback theory. In *IEE Proceedings D (Control Theory and Applications)*, volume 129, 215–226. IET.
- Jahangeer, K., Tay, A.A., and Islam, M.R. (2011). Numerical investigation of transfer coefficients of an evaporatively-cooled condenser. *Applied Thermal Engineering*, 31(10), 1655–1663.
- Keel, L., Kim, Y., and Bhattacharyya, S. (2008). Ch. 6 transient response control via characteristic ratio assignment. In *Lecture note of the 17th IFAC World Congress Tutorial Workshop: Advances in Three Term Control, Seoul*.
- Li, B. and Alleyne, A.G. (2010). A dynamic model of a vapor compression cycle with shut-down and start-up operations. *International Journal of refrigeration*, 33(3), 538–552.
- Rasmussen, B. (2005). Dynamic modeling and advanced control of air conditioning and refrigeration systems.
- Sira-Ramírez, H., Cortés-Romero, J., and Luviano-Juárez, A. (2011). Robust linear control of nonlinear flat systems. In *Robust Control, Theory and Applications*. InTech.